Lys49 myotoxin from the Brazilian lancehead pit viper elicits pain through regulated ATP release

Chuchu Zhang[a], Katalin F. Medzihradszky[b], Elda E. Sánchez[c,d], Allan I. Basbaum[e], and David Julius[a,1]

[a]Department of Physiology, University of California, San Francisco, CA 94158; [b]Department of Pharmaceutical Chemistry, University of California, San Francisco, CA 94158; [c]National Natural Toxins Research Center, Texas A&M University-Kingsville, Kingsville, TX 78363; [d]Department of Chemistry, Texas A&M University-Kingsville, Kingsville, TX 78363; and [e]Department of Anatomy, University of California, San Francisco, CA 94158

Contributed by David Julius, January 31, 2017 (sent for review September 16, 2016; reviewed by Baldomero M. Olivera and Mark J. Zylka)

Pain-producing animal venoms contain evolutionarily honed toxins that can be exploited to study and manipulate somatosensory and nociceptive signaling pathways. From a functional screen, we have identified a secreted phospholipase A2 (sPLA2)-like protein, BomoTx, from the Brazilian lancehead pit viper (*Bothrops moojeni*). BomoTx is closely related to a group of Lys49 myotoxins that have been shown to promote ATP release from myotubes through an unknown mechanism. Here we show that BomoTx excites a cohort of sensory neurons via ATP release and consequent activation of $P2X_2$ and/or $P2X_3$ purinergic receptors. We provide pharmacological and electrophysiological evidence to support pannexin hemichannels as downstream mediators of toxin-evoked ATP release. At the behavioral level, BomoTx elicits nonneurogenic inflammatory pain, thermal hyperalgesia, and mechanical allodynia, of which the latter is completely dependent on purinergic signaling. Thus, we reveal a role of regulated endogenous nucleotide release in nociception and provide a detailed mechanism of a pain-inducing Lys49 myotoxin from *Bothrops* species, which are responsible for the majority of snake-related deaths and injuries in Latin America.

Lys49 myotoxin | ATP release | pannexin | pain | purinergic receptor

Venoms from spiders, snakes, cone snails, and scorpions have evolved to produce a vast pharmacopoeia of toxins that modulate receptor or channel function as a means of producing shock, hemolysis, paralysis, and pain (1, 2). As such, venoms from these animals represent a rich potential source of potent and selective toxins that can be exploited to study and manipulate somatosensory and nociceptive signaling pathways. For example, toxins can directly target ion channels expressed by nociceptive sensory neurons to elicit or inhibit pain. Well-validated examples include toxins that target transient receptor potential (TRP) ion channels, acid-sensing ion channels (ASICs), and Na_v channels (3–8). However, the "toxinome" is incredibly diverse, and there are many pain-producing venoms for which the responsible toxins have not yet been identified.

In addition to targeting receptors and channels directly, algogenic toxins could also promote the synthesis and/or release of metabolites, transmitters, or second messengers that activate primary afferent nociceptors. Although this could occur through indiscriminate actions of venom lipases and proteases that release cellular contents through tissue damage and cell death, more specific mechanisms may also exist. Their identification could reveal important new pathways by which exogenous or endogenous pain-producing agents mediate their effects.

To identify novel pain-producing toxins, we have exploited cultured sensory neurons as a facile in vitro platform for unbiased screening of crude venoms, optimizing conditions to reduce nonspecific cell damage so as to reveal toxins having specific cellular effects. With this approach, we have identified a toxin (BomoTx) from the Brazilian lancehead pit viper (*Bothrops moojeni*) found mainly in Brazil. BomoTx belongs to a group of secreted phospholipase A2 (sPLA2)-like proteins that have the conserved PLA2 fold but lack enzymatic activity, and is most closely related to so-called Lys49 myotoxins found in snake species within the *Crotalinae* subfamily (9). These toxins are devoid of phospholipase activity due to key enzymatic site mutation of Asp49 to Lys49, but promote release of ATP from myotubes through an as-yet uncharacterized mechanism (10–12). Similarly, we show that BomoTx lacks phospholipase activity and excites a cohort of sensory neurons through a mechanism involving ATP release and activation of $P2X_2$ and $P2X_3$ purinergic receptors. Furthermore, we provide pharmacological and electrophysiological evidence to support a role for pannexin hemichannels in mediating toxin-evoked nucleotide release. At the behavioral level, injection of BomoTx into the mouse hind paw elicits nonneurogenic inflammatory pain, thermal hyperalgesia, and mechanical allodynia. The latter is completely dependent on purinergic signaling. Together, these findings elucidate a detailed mechanism by which a Lys49 myotoxin produces pain associated with envenomations common to Latin America (13).

Results

A Snake Toxin That Targets Somatosensory Neurons. To identify novel toxins that target nociceptors, we used live-cell calcium imaging to screen a library of 22 snake venoms for their ability to activate primary sensory neurons cultured from rat trigeminal ganglia (TG). Because many snake venoms contain cytolytic components, such as proteases and lipases (1, 14), initial screening of these samples resulted in cell injury and widespread calcium influx that masked the action of any specific components. To circumvent this problem, we first processed all crude venoms

Significance

Bites from venomous snakes can inflict substantial pain and inflammatory tissue damage. Snake phospholipase A2 (PLA2), and PLA2-like toxins that retain the PLA2 fold but lack enzymatic activity, are commonly found in snake venoms. In this study, we identify a PLA2-like toxin (BomoTx), from the Brazilian lancehead pit viper (*Bothrops moojeni*), that activates a subpopulation of somatosensory neurons that contribute to pain sensation. We show that BomoTx excites these neurons by stimulating the release of cellular ATP through a mechanism involving pannexin hemichannels. Consequent activation of purinergic receptors elicits acute pain, tissue inflammation, and pain hypersensitivity. Thus, we have elucidated the mechanism of action for a toxin from *Bothrops* snakes, which inflict a majority of bites in Latin America.

Author contributions: C.Z., A.I.B., and D.J. designed research; C.Z. and K.F.M. performed research; C.Z. and E.E.S. contributed new reagents/analytic tools; C.Z., K.F.M., A.I.B., and D.J. analyzed data; and C.Z. and D.J. wrote the paper.

Reviewers: B.M.O., University of Utah, Salt Lake City; and M.J.Z., University of North Carolina.

The authors declare no conflict of interest.

Data deposition: The sequence reported in this paper has been deposited in the GenBank database (accession no. KX856005).

[1]To whom correspondence should be addressed. Email: david.julius@ucsf.edu.

This article contains supporting information online at www.pnas.org/lookup/suppl/doi:10.1073/pnas.1615484114/-/DCSupplemental.

www.pnas.org/cgi/doi/10.1073/pnas.1615484114

through a 50-kDa molecular mass cutoff filter to enrich for peptides and small proteins. Indeed, this eliminated background activities in more than half of the crude venoms examined. Among these, filtrates from *B. moojeni* (Brazilian lancehead) (Fig. 1*A*) robustly activated a subpopulation of TG neurons (Fig. 1*B*). Fractionation of this crude venom by reversed-phase (C_{18}) chromatography yielded a single active peak (Fig. S1*A*) that recapitulated activity observed with the crude venom.

To determine the toxin's identity, we analyzed purified toxin by MALDI-TOF mass spectrometry, revealing a single polypeptide with a molecular mass of 13,835 Da (Fig. S1*C*). The sample was then trypsin-digested and analyzed by liquid chromatography-tandem mass spectrometry (LC/MS/MS). Homology considerations [to National Center for Biotechnology Information (NCBI) accession nos. 17865560 and 17368325 and UniProt accession no. Q9PVE3] and manual de novo sequencing provided a tentative full-sequence determination, which was then used to clone the full-length (122-amino acid) cDNA from the Brazilian lancehead venom gland. Indeed, the amino acid sequence translated from the toxin's ORF was identical to the proposed sequence, and the molecular mass calculated from it matched the experimentally determined results, assuming the presence of disulfide bridges. This species, which we call BomoTx, is a PLA2-like toxin whose pattern of cysteine residues classifies it specifically within a group known as Lys49 myotoxins (Fig. S1*J*) (9). Like other members of this myotoxin family, BomoTx has a lysine in place of a critical aspartate residue within the latent enzymatic pocket, and thus has retained the compact and stable fold of a PLA2-like protein but is devoid of catalytic activity (Fig. S1*B*).

BomoTx elicited two types of responses in neurons: large, sustained calcium signals in one group of TG neurons (Fig. 1*C*), and small, transient signals in a separate subpopulation (Fig. 1*D*). In addition, we also observed some calcium responses in fibroblasts, the majority of which were in the vicinity of neurons that exhibited sustained calcium signals (Fig. 1*E* and Fig. S1*H*). These responses were evoked by BomoTx alone, as digested BomoTx no longer activated any neurons (Fig. S1 *D–G*). Because BomoTx closely resembles Lys49 myotoxins (Fig. S1*J*), which are reported to cause ATP release from muscle cells (10), we wondered whether ATP signaling is involved in the responses we observed. Coapplication of ATP diphosphohydrolase apyrase eliminated transient toxin-evoked responses in both neurons and fibroblasts (Fig. 1 *G* and *H*) but not sustained responses in neurons (Fig. 1*F*). We conclude that ATP release is, indeed, required for transient toxin-evoked responses.

To more fully categorize these BomoTx-sensitive populations, we examined overlap between toxin-evoked responses and other functional or histological markers (Fig. S1*I*). Of the transient responders (Fig. 1*J*), most responded to ATP and α,β-MeATP (87.0 ± 12.1% and 93.8 ± 8.8%, respectively), which activate homomeric and heteromeric $P2X_3$ and $P2X_{2/3}$ purinergic receptors. A substantial percentage of transient responders also responded to agonists for TRPV1, TRPA1, TRPM8, and/or $Na_v1.1$ channels, and most (72.0 ± 18.9%) bound the lectin IB4. Taken together, these results indicate that these small- to medium-diameter transiently responding populations of BomoTx-sensitive neurons consist of both nonpeptidergic C fibers as well as peptidergic Aδ fibers. In contrast, neurons showing sustained toxin responses exhibited minimal overlap with TRPV1 (17.6%) or TRPA1 (0%) agonists, and relatively few responded to ATP (27.3%) or α,β-MeATP (0%) (Fig. 1*I*). These sustained responders were also of larger diameter (Fig. 1*K*), suggesting that they correspond to nonnociceptive Aα/Aβ-neurons.

BomoTx-Evoked Transient Responses Are Mediated by Purinergic Signaling. To address the basis of the toxin sensitivity in transiently responding neurons, we carried out whole-cell patch-clamp analysis of cultured TG neurons, which revealed a toxin-evoked inwardly rectifying current (Fig. 2*A*). Consistent with our pharmacological profiling by calcium imaging, extracellular ATP could invariably elicit currents in these neurons (Fig. 2*B*). Moreover, Ro51, a specific blocker of $P2X_3$ and $P2X_{2/3}$ ionotropic subtypes (15), reduced toxin-evoked responses by 72.2 ± 5.3% (Fig. 2*B*).

Does BomoTx elicit its response by activating P2X receptors directly, or by promoting release of ATP? To address this question, we first asked whether the toxin elicits membrane currents in transfected HEK293 cells expressing $P2X_2$ and/or $P2X_3$ receptors. No responses were observed (Fig. 2*C*), nor did the toxin shift dose–response curves for ATP (Fig. S2*A*), indicating that BomoTx is not a direct purinergic receptor agonist or modulator. Hence, the toxin likely promotes release of ATP to activate transient responses in specific sensory neurons that express purinergic receptors.

If ATP-evoked activation of P2X receptors accounts for BomoTx sensitivity in transiently responding neurons, ectopic expression of these channels in sensory neurons should increase the prevalence of toxin-responsive cells. We therefore transduced embryonic rat dorsal root ganglia (DRG) neurons with lentivirus carrying the full-length rat $P2X_2$ cDNA. After 7 d of expression, >95% of neurons responded to ATP or α,β-MeATP, compared with <20% in vector-infected or uninfected control cultures (Fig. 2*D*), demonstrating efficient ectopic expression of P2X receptors. Under these circumstances, BomoTx sensitivity was also more prevalent (20.12%) compared with controls (2.98%). Interestingly, activated neurons tended to cluster, supporting a possible ATP release and signaling mechanism. Furthermore, application of apyrase attenuated these transient BomoTx-evoked responses to 1.71% (Fig. 2*D* and Fig. S2*B*) but not sustained responses. Together, these results support the notion that BomoTx excites a subpopulation of sensory neurons by promoting release of ATP, followed by activation of $P2X_2$ and/or $P2X_3$ receptors.

BomoTx-Induced ATP Release Requires Hemichannels. In the lentiviral transduced embryonic DRG cultures, >99% of the cells are postmitotic neurons (Fig. S3*A*), and thus extracellular ATP could be released from neurons. Because BomoTx produces a sustained calcium response within a subpopulation of neurons that do not show sensitivity to apyrase, we hypothesized that these neurons might be the source of ATP release.

As noted above, BomoTx lacks PLA2 enzymatic activity, and thus loss of membrane integrity through lipase action is unlikely to be the cause of ATP release. Moreover, BomoTx was cytotoxic only at relatively high concentrations (Fig. S2*D*), far exceeding that required for repetitive transient responses. BomoTx also demonstrated specificity toward neurons and myotubes, as it failed to elicit calcium responses in a variety of other cell types, including glia-derived cell lines, smooth muscle cells, myeloblast-derived cell lines, and HEK293 cells (Fig. S2*E*). Taken together, these findings suggest that ATP release is not due to nonspecific cell damage or death.

In considering more specific mechanisms of toxin-evoked ATP release, we asked whether this could involve hemichannels or neuronal vesicles, which represent two main candidates for mediating nonlytic mechanisms of nucleotide release (16). First, we tested the effects of the vesicle release inhibitors *N*-ethylmaleimide and monensin, neither of which affected BomoTx-evoked responses (Fig. S3*B*). In addition, DRG neurons transduced with lentivirus carrying the long chain of tetanus toxin did not show reduced toxin sensitivity. Thus, a vesicular mechanism does not seem to underlie toxin-evoked ATP release.

We next asked whether blockers of pannexin and connexin hemichannels, such as carbenoxolone (CBX), niflumic acid (NFA), or flufenamic acid (FFA), could attenuate toxin sensitivity. Indeed, all of these agents dose-dependently reduced the number of BomoTx-sensitive neurons (Fig. S3 *C* and *D*); furthermore,

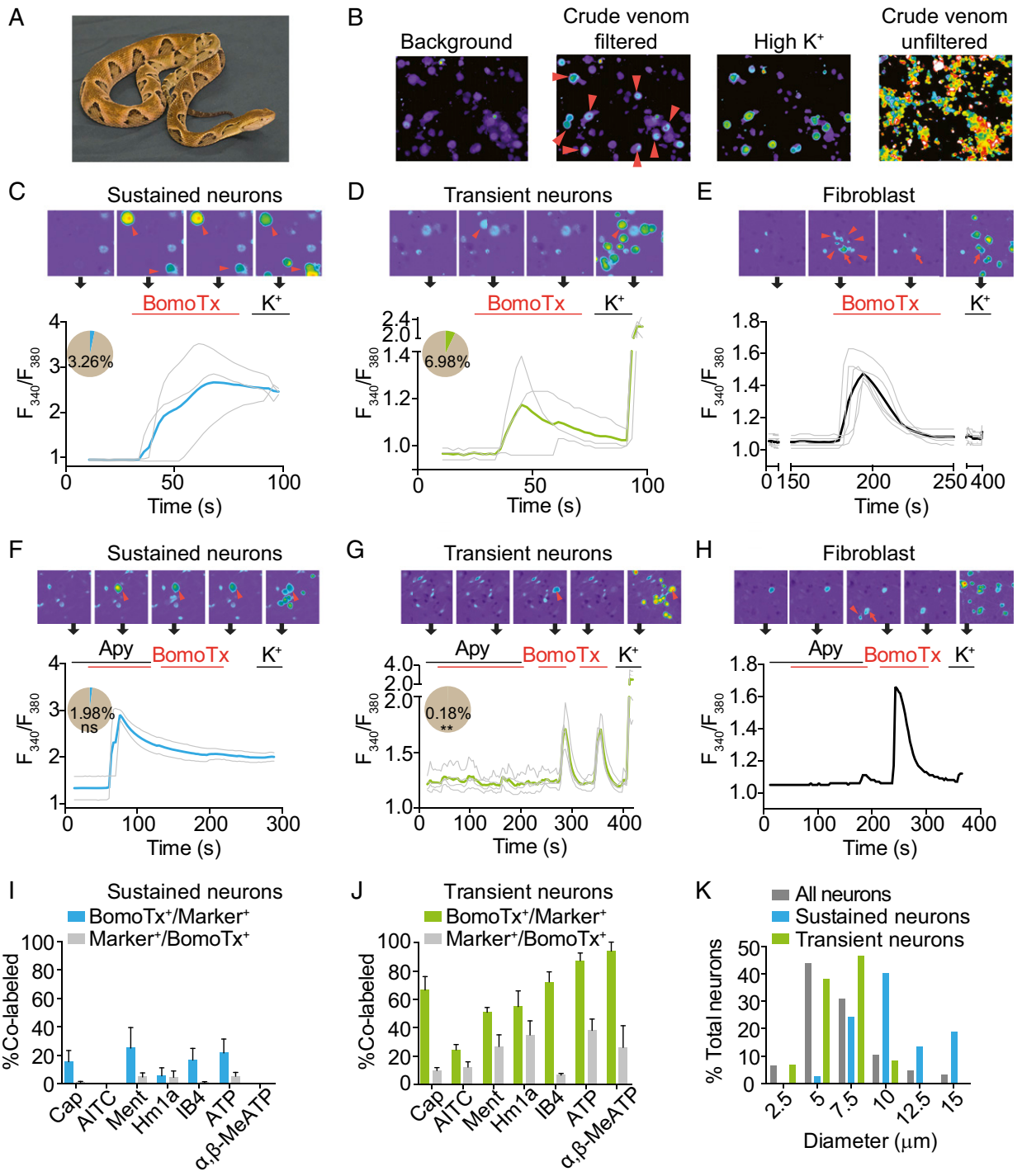

Fig. 1. BomoTx activates two distinct subpopulations of sensory neurons. (*A*) Brazilian lancehead, *B. moojeni*. Image courtesy of Texas A&M University, Kingsville, Office of Marketing and Communications. (*B*) Representative screen using ratiometric calcium imaging of cultured rat TG neurons. Crude snake venoms were analyzed before and after a filtration cleanup step to reveal, in some cases, specific responses by a subset of neurons (arrowheads). Subsequent response to high (150 mM) extracellular K^+ reveals all neurons in the field. (*C* and *D*) BomoTx (1 μM) elicited two types of responses characterized by large, sustained calcium responses in one group (*C*, pie chart blue slice, 3.26%) and small, transient calcium responses in another group (*D*, pie chart green slice, 6.98%). Representative images are shown above each trace, where arrowheads indicate BomoTx-sensitive neurons. (*E*) Nonneuronal cells (arrowheads) were activated in the vicinity of BomoTx-sensitive neurons showing sustained responses (arrows). They are characterized by transient calcium elevation with no response to high K^+. (*F* and *G*) Averaged calcium imaging traces of sustained (*F*, pie chart blue slice, 1.98%) and transient (*G*, pie chart green slice, 0.18%) BomoTx-sensitive neurons when apyrase (Apy; 20 U) was coapplied with the toxin. The number in *F* is not significantly different from that in *C*, whereas the number in *G* is significantly less than in *D*. $^{**}P < 0.01$, one-way ANOVA with post hoc Tukey's test. ns, not significant. (*H*) Responses by nonneuronal cells (arrowhead) are seen only in the absence of apyrase and in close proximity to BomoTx-sensitive sustained neurons (arrow). (*I* and *J*) Quantification of toxin-responsive sustained (*I*) and transient (*J*) cells in P0 TG cultures showing the percentage of toxin-sensitive cells that also responded to other agonists [10 nM capsaicin, 1 μM allyl isothiocyanate (AITC), 100 μM menthol, 1 μM Hm1a, 100 μM ATP, 30 μM α,β-MeATP] or bind the lectin IB4, and vice versa ($n = 3$ to 10). (*K*) Size distribution of all P0 TG neurons (gray; 125 neurons counted) and BomoTx-sensitive sustained (blue; 37 neurons counted) or transient (green; 60 neurons counted) neurons. All data represent mean ± SEM.

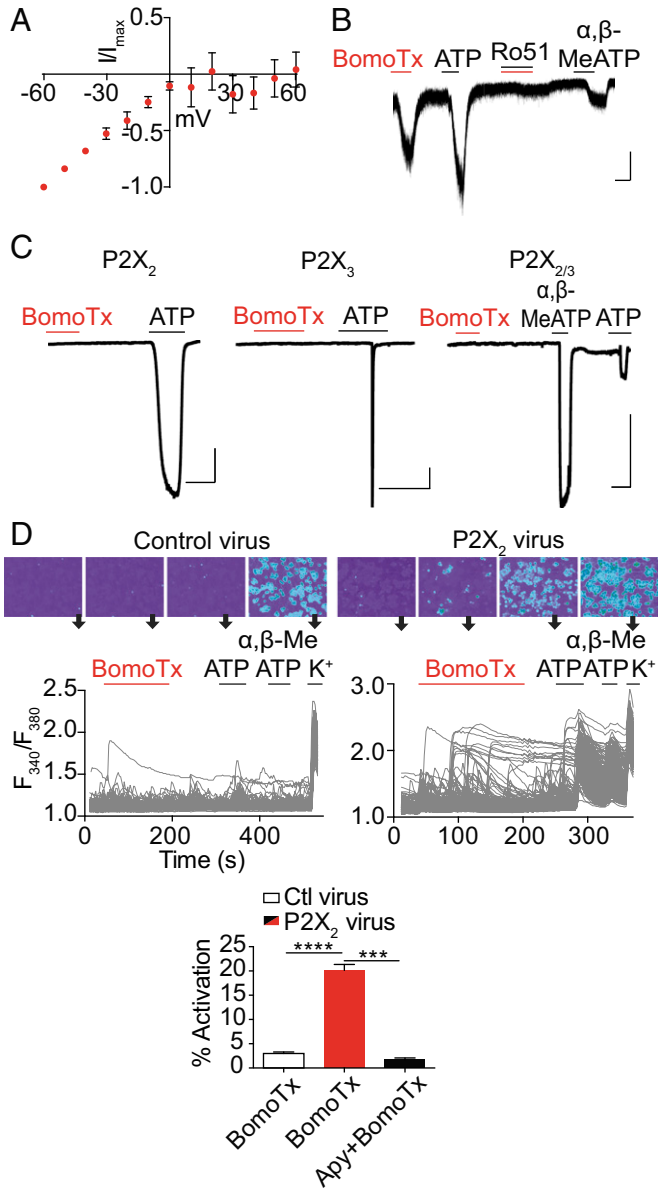

Fig. 2. BomoTx-induced transient responses are mediated by ATP. (*A*) Representative current–voltage relationship of BomoTx (1 μM)-evoked conductance from transiently activated TG neurons (whole-cell configuration; baseline-subtracted; each trace normalized to the current at −60 mV) demonstrates inwardly rectified currents that reverse at 0 mV ($n = 3$). (*B*) Representative whole-cell voltage-clamp experiments on TG neurons showing that Ro51 (100 nM) blocks BomoTx-evoked current. The same neurons also respond to ATP (100 μM) and α,β-MeATP (30 μM) ($n = 8$). (Vertical scale bars, 50 pA; horizontal scale bars, 10 s.) $V_{hold} = -60$ mV. (*C*) BomoTx does not directly activate HEK cells expressing rat $P2X_2$, $P2X_3$, or $P2X_{2/3}$ channels ($n = 7$ to 11). (Vertical scale bars, 0.5 nA; horizontal scale bars, 10 s.) (*D*) Embryonic DRG culture transduced with lentivirus expressing rat $P2X_2$ (*Top Right*) shows a significantly increased percentage of BomoTx-responsive cells (20.12%, $n = 30$) compared with uninfected control culture (*Top Left*) (2.98%, $n = 20$). Responses to ATP (100 μM) or α,β-MeATP (30 μM) were also increased in $P2X_2$-transduced cultures (*Middle*). Each trace represents an individual neuron ($n > 300$) with representative images shown above. Activities are quantified (*Bottom*). Apyrase (20 U) significantly reduces BomoTx-induced calcium responses in $P2X_2$-transduced culture (1.71%, $n = 3$). $^{***}P < 0.001$, $^{****}P < 0.0001$, one-way ANOVA with post hoc Tukey's test. Data are shown as mean ± SEM.

blockade at low CBX concentrations is indicative of a role for pannexin channels. Consistent with this, low concentrations of CBX also blocked ATP release in postnatal day (P)0 TG cultures (Fig. 3*A*). Taken together, we conclude that BomoTx elicits neuronal ATP release through a hemichannel-mediated pathway likely involving pannexins.

We then investigated whether BomoTx-induced pannexin opening underlies sustained toxin responses. Pannexins pass large molecules such as the dye YO-PRO-1, enabling us to ask whether pannexin opening correlates with sustained toxin-evoked calcium responses. In fact, we observed 93% overlap of these responses (Fig. 3*B*). Importantly, CBX-sensitive currents were also detected in these neurons, but not those exhibiting transient activation by BomoTx (Fig. 3*C*). Furthermore, pannexin itself is not sensitive to BomoTx, as HEK293 cells expressing pannexin 1, with or without pannexin 2, show no response to BomoTx (Fig. S3 *E* and *F*). These results suggest that BomoTx indirectly elicits pannexin opening and release of ATP, thus activating $P2X_2/X_3$ receptors and giving rise to transiently responding sensory neurons. Consistent with this mechanism, cells with YO-PRO-1 uptake (indicating a sustained toxin-evoked population) (Fig. 3 *D* and *I*) demonstrated intracellular calcium release caused by BomoTx. These responses could induce various magnitudes of store-operated calcium entry (SOCE) (Fig. 3*D*) and were attenuated by pretreatment with thapsigargin and U73122 (Fig. 3 *F* and *G*), suggesting that BomoTx promotes release of calcium from intracellular stores via PLC pathways in these cells. On the other hand, toxin-evoked apyrase-sensitive transient responses depended on extracellular calcium, and were not accompanied by YO-PRO-1 uptake (Fig. 3 *D*, *E*, *H*, and *I*).

Thus, we conclude that (Fig. 3*J*) BomoTx evokes intracellular calcium release from a specific population of sensory neurons. Subsequent signaling events lead to hemichannel pannexin opening to release ATP to the extracellular environment. Released ATP then activates purinergic signaling in sensory neurons through $P2X_2$ and/or $P2X_3$, which are the major purinergic receptors on these cells. Because pharmacological blockade of these channels does not eliminate all transient responses, other P2X and/or P2Y receptors likely contribute to residual toxin sensitivity in some neural and nonneural cells (17).

BomoTx Evokes Pain and Produces Thermal and Mechanical Sensitization. Because BomoTx excites presumptive nociceptors, we asked whether it produces pain-like behaviors when injected into the mouse hind paw. Indeed, nocifensive responses were observed (Fig. 4*A*), including robust licking of the injected paw that was accompanied by edema (Fig. S4*A*). Abundant Fos expression was induced in superficial laminae of the ipsilateral dorsal spinal cord (Fig. 4 *B* and *C*), consistent with activation of nociceptive pathways. In contrast, BomoTx did not induce expression of ATF-3, a marker of nerve damage, in lumbar DRG neurons (Fig. S4*E*), consistent with our cellular data suggesting that toxin-evoked responses are not simply a consequence of neuronal death.

We next asked whether BomoTx promotes persistent pain. We injected toxin into the hind paw at a dose insufficient to generate acute pain, and after 30 min assessed sensitivity to thermal or mechanical stimuli. We observed significant hypersensitivity to heat as evidenced by decreased paw withdraw latency in the Hargreaves assay (Fig. 4*D*), as well as mechanical hypersensitivity as measured by decreased paw withdraw threshold in the von Frey assay (Fig. 4*E*).

BomoTx-induced pain and sensitization were accompanied by paw edema, and we therefore asked whether TRPV1-positive neurons, which play a key role in heat hypersensitivity and neurogenic inflammation, contribute to toxin-evoked nocifensive behaviors. In animals in which the central projections of TRPV1-positive fibers were ablated by spinal (intrathecal) capsaicin injection (Fig. S4 *B* and *C*), BomoTx-evoked acute pain was significantly reduced (Fig. 4*A*), as was Fos expression in the spinal cord (Fig. 4 *B* and *C*). These animals also showed complete loss of toxin-induced heat hypersensitivity (Fig. 4*D*). In contrast, BomoTx-evoked mechanical hypersensitivity was unaffected (Fig. S4*D*), consistent

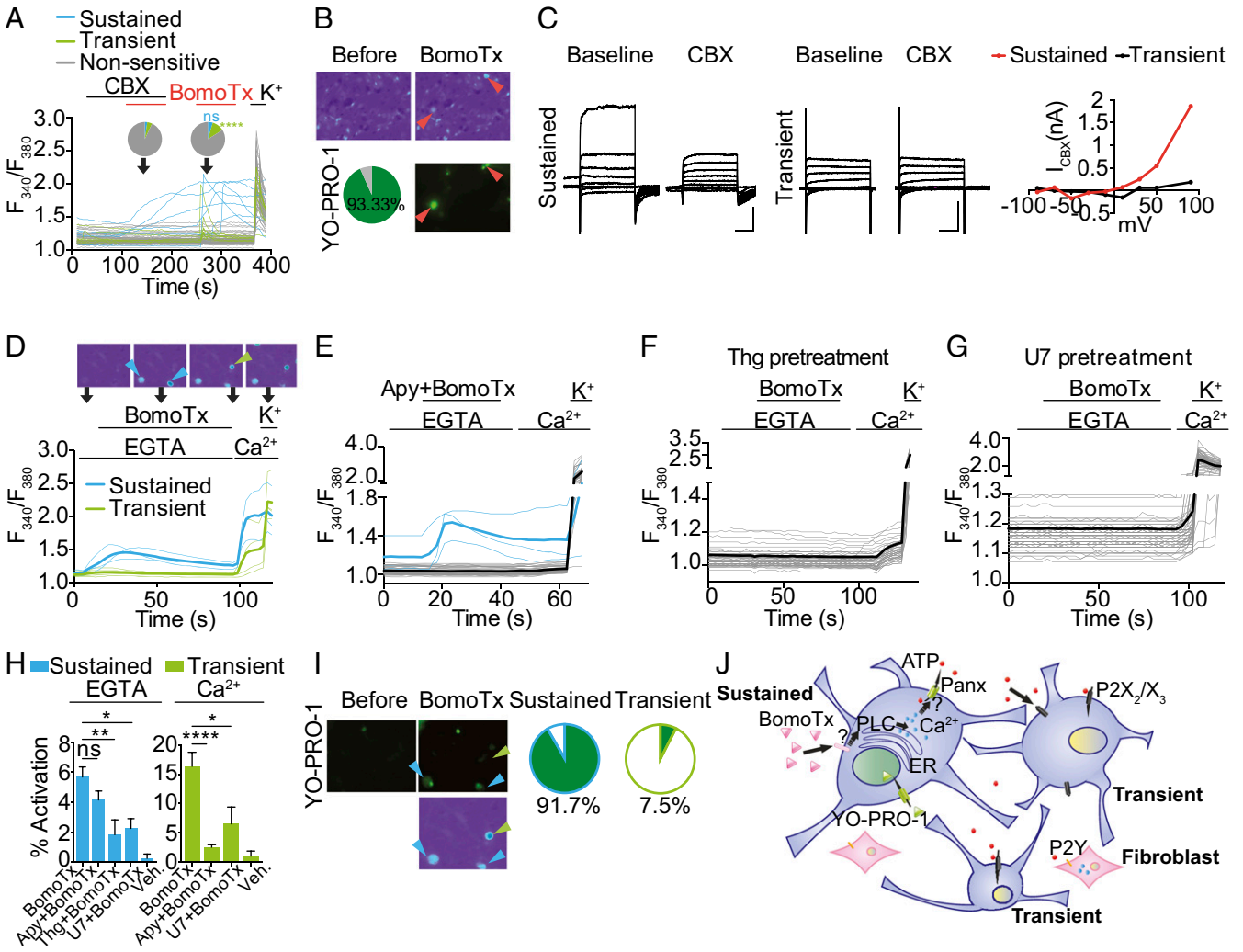

Fig. 3. BomoTx-induced ATP release requires hemichannels. (*A*) Calcium imaging traces showing examples of BomoTx (1 μM) application in P0 mouse TG culture (>70 neurons) with and without CBX (10 μM). Blue traces and pie chart slice indicate sustained neurons (2.33% with CBX and 4.57% without CBX); green traces and pie chart slice indicate transient neurons (4.65% with CBX and 11.45% without CBX) ($n = 5$). ****$P < 0.0001$, one-way ANOVA with post hoc Tukey's test. (*B*) Representative images of neurons with sustained calcium responses (arrowheads) compared with those subsequently exhibiting YO-PRO-1 (0.1 μM) uptake, showing complete (93.3 ± 16.3%) overlap ($n = 6$). (*C*, *Left* and *Middle*) Whole-cell patch recordings from neurons showing sustained or transient calcium responses immediately after toxin application. Eighty percent (4/5) of sustained neurons showed a CBX-sensitive current, compared with none (0/5) of the transiently activated cells. Voltage steps are from −90 to 90 mV with a 20-mV increment; the holding potential is −70 mV. (Vertical scale bars, 1 nA; horizontal scale bars, 100 ms.) (*C*, *Right*) Current–voltage relationship of CBX-sensitive currents in BomoTx-evoked transient and sustained neurons. I_{CBX} is calculated by subtracting the steady-state current at each voltage step from that in the presence of CBX. (*D*) Calcium imaging of BomoTx-evoked responses in the absence and presence of extracellular calcium. With EGTA and no extracellular calcium, a group of neurons (blue traces and arrowheads; the thick trace is the average of all blue traces) was activated; adding extracellular calcium subsequently activated another group of neurons (green traces and arrowheads). Note that addition of extracellular calcium also activates SOCE in the first group of neurons ($n = 20$). (*E*) Coapplication of apyrase (20 U) and BomoTx did not affect toxin-evoked intracellular calcium transients and SOCE (blue traces) but reduced the population of cells responding to subsequent extracellular calcium addition (gray traces) ($n = 32$). (*F*) Pretreatment with thapsigargin (Thg; 2 μM, 5 min) in the absence of extracellular calcium abolished all BomoTx responses. Subsequent addition of extracellular calcium activated SOCE in all cells ($n = 12$). (*G*) Pretreatment with U73122 (U7; 10 μM, 5 min) in the absence of extracellular calcium abolished all BomoTx responses. (*H*) Quantification of the percentage of the calcium responses evoked by BomoTx under different calcium conditions. *$P < 0.05$, **$P < 0.01$, ****$P < 0.0001$, one-way ANOVA with post hoc Tukey's test. (*I*) YO-PRO-1 staining immediately after BomoTx application in the absence and then presence of extracellular calcium. The calcium imaging example is from *D*; blue and green arrowheads indicate cells with intracellular calcium release and extracellular calcium responses, respectively (*Left*). Note that only cells with intracellular calcium release have YO-PRO-1 staining. Pie charts show the percentage of YO-PRO-1–positive neurons (green) for those exhibiting BomoTx-evoked intracellular calcium release (*Middle*) versus extracellular calcium influx (*Right*) ($n = 4$). (*J*) Proposed mechanism of BomoTx action in neurons. BomoTx targets sensory neurons through an unknown receptor, which activates intracellular calcium release, leading to subsequent pannexin hemichannel opening, YO-PRO-1 permeation, and ATP release. The released ATP then activates sensory neurons that express ionotropic $P2X_2$ and $P2X_3$ receptors, as well as P2Y metabotropic receptors on fibroblasts.

with the fact that TRPV1-expressing fibers are essential for thermal, but not mechanical, hypersensitivity (18, 19).

Because ATP-evoked $P2X_2/X_3$ responses (i.e., transiently responding neurons) constitute a major component of BomoTx signaling, we asked whether $P2X_2/X_3$ activation also contributes to the observed behavioral responses. We compared toxin-evoked nocifensive behaviors, as well as heat and mechanical sensitization, in both WT and $P2X_2/P2X_3^{dbl-/-}$ mice (20, 21). Strikingly, elimination of $P2X_2$ and $P2X_3$ significantly attenuated mechanical sensitization (Fig. 4*E*) without diminishing acute nocifensive behaviors (Fig. 4*A*)

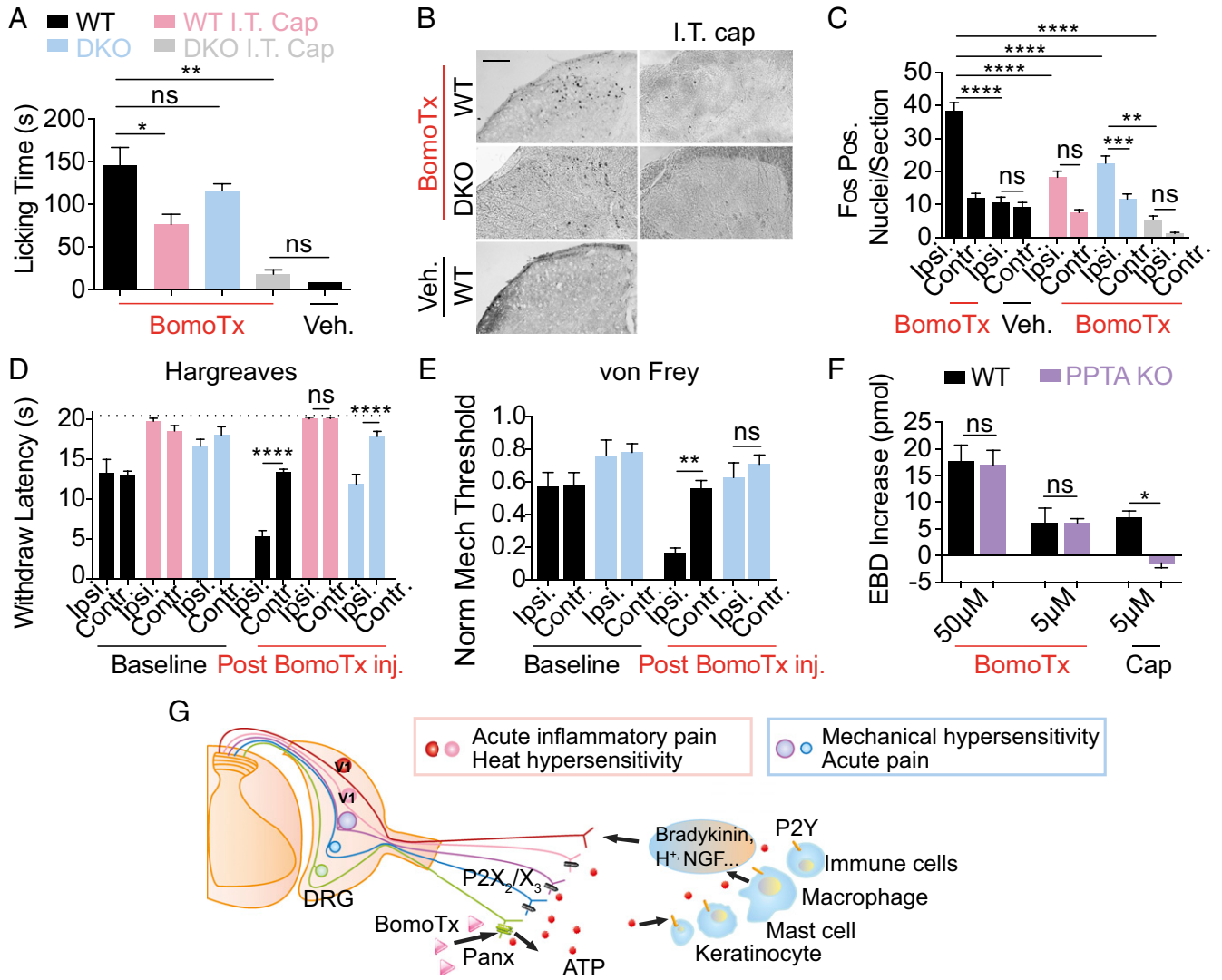

Fig. 4. BomoTx evokes pain and produces thermal and mechanical hypersensitivity. (*A*) Comparison of licking behavior following intraplantar injection of BomoTx (50 μM in 20 μL 0.1% BSA) ($n = 7$) versus vehicle ($n = 4$). Nocifensive behavior was not significantly reduced in $P2X_2/P2X_3^{dbl-/-}$ (DKO) mice ($n = 6$) but was significantly decreased after ablation of TRPV1-expressing terminals in the spinal cord by intrathecal capsaicin (I.T. cap) injection in WT($n = 10$) and DKO mice ($n = 3$). (*B* and *C*) Quantification and representative images of Fos protein immunostaining in superficial laminae of spinal cord sections from toxin-injected mice ipsilateral (Ipsi.) or contralateral (Contr.) to the injected hind paw (sections: $n = 80$ for WT and DKO, $n = 30$ for I.T. cap, and $n = 20$ for I.T. cap DKO and control). (Scale bar, 100 μm.) (*D*) Latency of paw withdrawal from noxious heat stimulus measured in WT ($n = 6$), DKO ($n = 6$), and I.T. cap ($n = 7$) mice 15 min after BomoTx (5 μM) or vehicle ($n = 3$) injection. (*E*) Mechanical threshold for WT or DKO mice ($n = 8$ each) 15 min after vehicle or BomoTx intraplantar injection. (*F*) Evans blue dye extravasation measured in BomoTx- or capsaicin (5 μM)-injected paw compared with contralateral controls in WT and $PPTA^{-/-}$ mice ($n = 3$ for all BomoTx injections; $n = 7$ for WT cap injection). (*G*) Proposed mechanism of BomoTx-evoked pain. BomoTx releases ATP from nerve endings through hemichannels, directly activating P2X- and/or P2Y-expressing sensory neurons, as well as nonneural cells (e.g., keratinocytes, mast cells, local immune cells) that release inflammatory mediators (such as bradykinin, H^+, and more ATP), in turn activating sensory nerve fibers. Activation and sensitization of TRPV1-positive fibers produce acute inflammatory pain and thermal hypersensitivity, whereas activation of $P2X_2$ and $P2X_3$ fibers elicits acute pain and mechanical hypersensitivity. For all, $^*P < 0.05$, $^{**}P < 0.01$, $^{***}P < 0.001$, $^{****}P < 0.0001$, one-way ANOVA with post hoc Tukey's test. Data are shown as mean ± SEM.

or thermal sensitization (Fig. 4*D*). When $P2X_2/P2X_3^{dbl-/-}$ mice were treated with intrathecal capsaicin, acute toxin-evoked nocifensive behavior was completely lost (Fig. 4*A*), demonstrating that TRPV1- and $P2X_2/P2X_3$-expressing fibers together account for all toxin-evoked acute behaviors.

BomoTx Promotes Nonneurogenic Inflammation. BomoTx causes ATP release from neurons, which can target many other cell types in the nerve terminals, such as keratinocyte, macrophage, and immune cells (22). We therefore asked whether toxin-induced inflammation and paw edema are neurogenic (i.e., require initial activation of substance P-expressing sensory nerve fibers). We measured toxin-evoked paw edema and Evans blue dye (EBD) uptake in preprotachykinin A-deficient mice ($PPTA^{-/-}$), which do not exhibit neurogenic inflammation (23). As expected, these animals show minimal paw edema and EBD uptake after capsaicin injection (Fig. 4*F* and Fig. S4 *F* and *G*). However, in both WT and $PPTA^{-/-}$ mice, BomoTx induced robust paw swelling and EBD uptake in the ipsilateral paws, at both high and low toxin doses (Fig. 4*F* and Fig. S4 *F* and *G*).

Taken together (Fig. 4*G*), these observations suggest that BomoTx produces swelling and edema through a nonneurogenic mechanism involving ATP action on immune or other nonneural cell types in the local tissue environment. ATP and other inflammatory agents act on TRPV1-positive neurons to elicit

acute pain behaviors (24) and heat hypersensitivity. Furthermore, ATP signaling through $P2X_2$ and $P2X_3$ receptors on TRPV1-negative sensory neurons contributes to toxin-evoked mechanical sensitization, consistent with the fact that non-TRPV1 Aδ-fibers, which also express $P2X_2$ and $P2X_3$, are involved in mechanical hypersensitivity (7, 25).

Discussion

We have identified a pain-inducing Lys49 myotoxin, BomoTx, which activates the pannexin pathway and two groups of sensory neurons. These groups include (*i*) a transiently responding cohort representing nonpeptidergic C and Aδ-fibers whose activation depends on P2X receptors, and (*ii*) a cohort in which toxin-evoked sustained responses require intracellular calcium signaling and involve activation of pannexin hemichannels. We propose that BomoTx elicits nucleotide release from neurons showing sustained responses through hemichannel activation, thereby promoting activation of P2X receptors on transiently responding neighbors. We also observed BomoTx-evoked nocifensive behaviors, including acute pain accompanied by nonneurogenic inflammation, as well as thermal hypersensitivity—both mediated mainly through TRPV1-positive fibers. Furthermore, the toxin produced mechanical allodynia that required purinergic signaling through TRPV1-negative, $P2X_2$-, and/or $P2X_3$-positive neurons, likely representing Aδ-fibers. Together, these findings support a role for regulated release of endogenous nucleotides in nociception, as well as involvement of ionotropic P2X receptors in mechanical hypersensitivity.

BomoTx Relationship to Lys49 Myotoxins. Lys49 myotoxins are a family of proteins that displays myotoxicity despite being catalytically inactive. BomoTx contains key protein sequence features of Lys49 myotoxins and also activates C2C12 myotubes (but not C2C12 myoblasts), thereby a true member of the family of Lys49 myotoxins. It has been reported that ATP release contributes to Lys49 myotoxin-induced myotoxicity, but detailed mechanisms remain unknown and it is unclear how toxin specificity toward myotubes (but not myoblasts and other cell types) is achieved. One hypothesis is that Lys49 myotoxins interact with membrane receptors that determine their specificity of action, but to date no such receptors have been identified. Here we describe a potential pathway underlying BomoTx action that involves intracellular calcium signaling and pannexin hemichannel activation, providing evidence that ATP release by this family of snake toxins occurs through a specific cellular signaling pathway, rather than indiscriminate cellular injury. Moreover, we show that BomoTx induces Ca^{2+} responses in a subset of sensory and hippocampal neurons, as well as myotubes, but not other cell types tested, and the time course of ATP release is much faster (within 1 min) than that reported for other membrane-damaging toxins (5 to 20 min) (26, 27). Hence, at lower concentrations, BomoTx exerts biological functions specific to neurons (or muscles) that do not require membrane disruption. It is possible that this specificity is achieved by the presence of different signaling components (receptors, calcium release mechanisms, pannexin). Still, as in the case of Lys49 myotoxins, the exact mechanism underlying cellular specificity and/or the existence of a bona fide BomoTx receptor remains unknown.

Involvement of Hemichannels in Toxin-Evoked ATP Release. Pannexin 1 can be activated by several stimuli, including caspase activation (28), Rho signaling (29), and mechanical stretch (30). Here we observed BomoTx-evoked intracellular Ca^{2+} release via the PLC pathway and YO-PRO-1 uptake in cells that also display CBX-sensitive pannexin currents. Hence, we suggest that BomoTx-induced intracellular Ca^{2+} elevation occurs upstream of pannexin activation. However, because neurons exhibiting transient toxin-evoked or ATP-evoked Ca^{2+} influx do not develop pannexin currents, consistent with previous observations (29), increased cytoplasmic Ca^{2+} per se may not be sufficient to activate pannexin currents. As such, we hypothesize that additional signaling steps are required to connect BomoTx-induced Ca^{2+} increases to pannexin activation.

Distinct Fiber Types Contribute to BomoTx-Evoked Acute and Persistent Pain. *Bothrops* species are responsible for the majority of snake-related deaths and injuries in Latin America. Pain and tissue inflammation are hallmarks of viperid snake bites; other common symptoms include blisters, necrosis, and hemorrhage (13, 31, 32). *B. moojeni* venom contains a complex mixture of metalloproteinases (33, 34), serine proteases (35), L-amino acid oxidases (36), acidic PLA2s (37), and Lys49 myotoxins (38), all of which likely contribute to the envenomation symptoms. Here we show that a specific venom component, a Lys49 myotoxin, can directly elicit pain and inflammation as well as mechanical and heat hypersensitivity. Because BomoTx action appears to be neural-specific and does not directly promote nerve damage, we hypothesize that these physiological and behavioral effects of BomoTx are initiated by ATP release from BomoTx-sensitive primary afferent nerve terminals. The ATP released can activate $P2X_2$- and/or $P2X_3$-expressing nociceptors, as well as P2Y-expressing nonneural cell types, as observed in our culture system, where ATP released from neurons activates nearby fibroblasts. Subsequent release of inflammatory effectors (including purines) (22) can then act back on nociceptors to generate inflammatory pain and hypersensitivity. For example, stimulation of TRPV1-positive fibers produces heat hypersensitivity, whereas activation of $P2X_2/P2X_3$-expressing fibers elicits mechanical hypersensitivity, consistent with roles for these nociceptor subtypes in thermal and mechanical pain, respectively (25, 39).

Materials and Methods

Venom Screen. Crude snake venoms were provided by the National Natural Toxins Research Center, Texas A&M University-Kingsville. Approximately 10 mg of lyophilized crude snake venoms was dissolved in 200 μL water and filtered through centrifugal filters with a membrane molecular mass cutoff of 50 kDa (Millipore). Filtered venoms were buffered in isotonic solution (140 mM NaCl, 5 mM KCl, 2 mM $CaCl_2$, 2 mM $MgCl_2$, 10 mM glucose, 10 mM Hepes, pH 7.4) for ratiometric calcium imaging in sensory neurons. Neurons were previously loaded with Fura-2 AM (Molecular Probes) for >1 h. Response to high extracellular potassium (150 mM KCl, 10 mM Hepes, pH 7.4) was used to identify neurons. Venoms causing robust neuronal responses were kept for further analysis. All calcium imaging responses were digitized and analyzed using MetaFluor software (Molecular Devices).

Toxin Purification. Crude *B. moojeni* venom was dissolved in water to 100 mg/mL, diluted threefold with 5% (vol/vol) acetonitrile containing 0.1% trifluoroacetic acid (TFA), filtered through a 0.1-μm centrifugal filter unit (Millipore), and fractionated by reversed-phase HPLC. Up to 25 mg venom was loaded onto a semipreparative C18 column (Vydac; 218TP510) and eluted with a 19-min linear gradient (15 to 70%; 3 mL/min). Solvent A was 0.1% TFA in water, and solvent B was 0.1% TFA in 90% acetonitrile. Fractions containing BomoTx were lyophilized, dissolved, diluted in 5% acetonitrile with 0.1% TFA, applied to an analytical C18 column (Vydac; 218TP54), and separated with a 20-min linear gradient (26 to 46%; 0.8 mL/min). All purifications were performed at room temperature. Purified fractions were lyophilized, dissolved in water, aliquoted, and stored at −80 °C. Protease (Sigma; P8811) digestion of the purified fractions was conducted at 37 °C for up to 24 h, and the protease was heat-inactivated at 85 °C for 15 min.

Sequence Determination. The freshly purified active fraction was mixed 1:1 (vol/vol) with sinapinic acid (10 mg/mL) and then spotted onto the target. Data were collected over a range of 1,000 to 20,000 *m/z* on an AXIMA Performance MALDI-TOF/TOF mass spectrometer (Shimadzu) in linear mode and calibrated using the ProteoMass Kit (Sigma). The molecular mass of the polypeptide was determined to be 13,835 Da. Only ions corresponding to this polypeptide were observed.

An aliquot of the fraction was diluted to feature a 20 mM NH_4HCO_3 concentration, the disulfide bridges were reduced with DTT (30 min, 60 °C),

and the free sulfhydryls were alkylated with iodoacetamide (30 min, room temperature). Tryptic digestion [2% (wt/wt) side chain-protected porcine trypsin; Promega] was performed at 37 °C for 5 h. The digest was analyzed by LC/MS/MS analysis using a Famos autosampler/Eksigent nanopump HPLC system directly linked to a QSTAR Elite (Sciex) quadrupole-orthogonal-acceleration-time-of-flight mass spectrometer. The peptides were fractionated on a homemade C18 column (100 μm i.d. × 150 mm) at a flow rate of 400 μL/min. Solvent A was 0.1% formic acid in water and solvent B was 0.1% formic acid in acetonitrile. The sample was injected onto the column at 5% solvent B and a linear gradient was developed to 40% B over 35 min. Data acquisition was performed in an information-dependent manner: The two most abundant multiply charged ions were fragmented after each MS survey scan. The collision energy was automatically adjusted according to the precursors' *m/z* and *z* values. Dynamic exclusion was enabled.

From the raw data, a peak list was generated using a Mascot script provided by the manufacturer (Sciex). ProteinProspector (prospector.ucsf.edu/prospector/mshome.htm) was used for the database search, with the following parameters: enzyme, trypsin; carbamidomethylation of Cys, fixed modification; acetylation of protein N termini, Met oxidation, and cyclization of N-terminal Gln residues, variable modifications; and mass error permitted, 200 and 300 ppm for precursor ions and fragments, respectively. First, we searched the SwissProt.2012.03.21 database, without species specification (535,248/535,248 entries searched), permitting only one missed cleavage to ascertain that there were no unexpected protein contaminations in the sample, and then a species-specific (*B. moojeni*) search was performed using the NCBInr.2011.01.09 database (27/12,679,686 entries searched), with three missed cleavages permitted to achieve the best possible sequence coverage.

The sequences identified unambiguously indicated that the active ingredient must be an unreported phospholipase. Homology considerations (to NCBI accession nos. 17865560 and 17368325 and UniProt accession no. Q9PVE3) and manual de novo sequencing led to a tentative full-sequence determination: SLVELGKMILQETGKNPVTSYGAYGCNCGVLGRGKPKDATDRCCYVHKCCYKKLTDCNPKKDRYSYSWKDKTIVCGENNSCLKELCECDKAVAICLRENLDTYNKKYKNNYLKPFCKKADPC.

The sequence was confirmed by translating the ORF. The calculated molecular mass 13,834 Da (with all Cys residues in disulfide bridges) shows good agreement with the experimentally determined value. The sequence information can be found in GenBank under accession no. KX856005.

When determining the protease (Sigma; P8811) digestion results, standards were mixed with the sample including angiotensin II (Sigma; A8846), ACTH fragment 18–39 (Sigma; A8346), insulin oxidized B chain (Sigma; I6154), insulin (Sigma; I6279), cytochrome *c* (Sigma; C8857), and apomyoglobin (Sigma; A8971).

BomoTx cDNA Cloning. Deduced sequences covering the mature BomoTx were used to clone full-length BomoTx cDNAs. RNA was extracted from one *B. moojeni* venom gland using TRIzol reagent (Invitrogen) and then isolated by chloroform extraction and isopropanol precipitation. A cDNA library was generated for use in 5′ and 3′ rapid amplification of cDNA ends (RACE) reactions using the SMARTer RACE cDNA Amplification Kit (Clontech). Degenerative primers were designed to amplify fragments of BomoTx sequences covering the 5′ and 3′ UTRs, which were sequenced after insertion into the TOPO vector (Invitrogen). The 5′ and 3′ UTR sequences were used to design specific primers to amplify the full-length cDNA. The cDNA-derived peptide sequence agreed with the observed molecular mass of the purified toxins, assuming the presence of disulfide bridges. sPLA2 activity was assessed using the $sPLA_2$ Assay Kit (Cayman Chemical).

Sensory Neuron Culture. Trigeminal ganglia were dissected from newborn (P0 to P3) C57BL/6 mice or rats and cultured for >12 h before calcium imaging or electrophysiological recording. Primary cells were plated onto coverslips coated with poly-L-lysine (Sigma; 0.01%) and laminin (Invitrogen; 10 μg/mL). Embryonic DRG cultures were generously provided by Jonah Chan, University of California, San Francisco (32). Embryonic cultures were maintained as described and transduced with freshly made lentivirus supernatant at days in vitro (DIV)4. Calcium imaging experiments were performed at DIV14.

Lentivirus Production. HEK293T cells were maintained in DMEH-21 medium with 10% FBS and penicillin/streptomycin in 5% CO_2 at 37 °C. Lentivirus was produced by transfecting HEK293T cells with FUGW-rat $P2X_2$, psPAX2, and pVSVG using FuGENE HD (Roche) according to the manufacturer's instructions.

Electrophysiology. TG neuron whole-cell recording extracellular solution contained 150 mM NaCl, 2.8 mM KCl, 1 mM $MgSO_4$, 2 mM $CaCl_2$, 10 mM Hepes, 290 to 300 mOsmol/kg (pH 7.4). The pipette solution contained 130 mM K-gluconate, 15 mM KCl, 4 mM NaCl, 0.5 mM $CaCl_2$, 1 mM EGTA, 10 mM Hepes, 280 to 290 mOsmol/kg (pH 7.2). For whole-cell recordings from HEK293 cells, the extracellular solution contained 150 mM NaCl, 2.8 mM KCl, 1 mM $MgSO_4$, 2 mM $CaCl_2$, 10 mM Hepes, 290 to 300 mOsmol/kg (pH 7.4). The pipette solution contained 130 mM Cs-$MeSO_3$, 15 mM CsCl, 4 mM NaCl, 5 mM BAPTA (1,2-bis(*o*-aminophenoxy)ethane-*N*,*N*,*N*′,*N*′-tetraacetic acid), 10 mM Hepes, 280 to 290 mOsmol/kg (pH 7.4). Whole-cell patch clamp of cultured mouse TG neurons and HEK293 cells was performed as described (4). Extracellular solution was perfused with or without toxins/drugs using a SmartSquirt Micro-Perfusion System (AutoMate). All recordings were performed using fire-polished glass electrodes with a resistance of 2 to 5 MΩ at room temperature (20 to 22 °C). Signals were amplified using an Axopatch 200B amplifier, digitized with a Digidata 1440A, and recorded using pCLAMP 10.2 software (Molecular Devices). For all DRG neurons the holding potential was −80 mV. Drugs used in the study were apyrase (Sigma), Ro51 (Tocris), ATP (Sigma), α,β-MeATP (Sigma), carbonoxolone (Sigma), niflumic acid (Tocris), flufenamic acid (Tocris), monensin (Tocris), *N*-ethylmaleimide (Sigma), YO-PRO-1 iodide (Thermo Fisher Scientific), thapsigargin (Tocris), U73122 (Sigma), Z-VAD-FMK (Tocris), and Evans blue dye (Sigma).

Behavior. Mice were bred and housed in accordance with University of California, San Francisco (UCSF) Institutional Animal Care and Use Committee (IACUC) guidelines. Two to five animals were housed together on a 12-h light/dark schedule with constant access to food and water. Behavioral experiments were approved by the UCSF IACUC and were in accordance with the NIH *Guide for the Care and Use of Laboratory Animals* (40) and the recommendation of the International Association for the Study of Pain. $P2X_2/P2X_3^{dbl-/-}$ mice were generously provided by Thomas E. Finger, University of Colorado School of Medicine, Denver, CO. Intraplantar injections (20 μL PBS + 0.1% BSA, with or without 50 μM BomoTx) were performed on adult (10- to 18-wk-old) mice. Nocifensive responses were recorded during a 20-min observation period immediately following intraplantar injections. Licking and lifting behavior was scored with the experimenter blinded to injection condition and experimental cohort. Hargreaves and von Frey tests were performed 15 min after intraplantar injection of 5 μM BomoTx to measure heat and mechanical sensitivity, respectively. Intrathecal capsaicin ablation was performed as previously described (19), and ablation was confirmed by hot plate test and histology. Evans blue dye (30 mg/kg) was administered retroorbitally into the mice retrobulbar sinus 1 min before intraplantar application of BomoTx (50 and 5 μM) or capsaicin (5 μM). Mice were euthanized 30 min after application of the stimulus. The skin of the hind paws was removed and the extravasated dye was extracted in formamide for 48 h at 65 °C in the dark and measured by using a spectrophotometer (620 nm). For ATF3 staining, mice hind paws were injected with 20 μL PBS + 0.1% BSA with 50 μM BomoTx, 5% formalin, or 30 μM α,β-MeATP. Mice were euthanized 2 d after the injection. Male and female mice were first considered separately in hind paw nocifensive response experiments. Both sexes showed significantly greater responses to toxin than vehicle control. Therefore, male and female behavioral responses were pooled and subsequent experiments were performed on both male and female mice.

Immunohistochemistry. Mice were deeply anesthetized with pentobarbital and then transcardially perfused with 10 mL of PBS followed by 10 mL of 10% neutral buffered formalin (NBF). Spinal cord lumbar sections or DRGs were dissected, postfixed in 10% NBF at room temperature for 2 h, cryoprotected in PBS with 30% (wt/vol) sucrose overnight at 4 °C, and embedded in OCT compound at −20 °C. Tissue was sectioned at 25 μm, thaw-captured on Diamond White Glass slides (Globe Scientific), and stored at −20 °C until use. Slides were incubated for 1 h at room temperature in a blocking solution consisting of PBS with 0.2% (vol/vol) Triton X-100 (Sigma), 0.1% BSA, and 2% normal goat serum. Slides were then incubated in primary antibody overnight at 4 °C and then washed in fresh PBS three times and incubated in secondary antibody for 1 h at room temperature in the dark. Sections were then washed in fresh PBS three times before mounting with ProLong Gold antifade reagent with DAPI (Life Technologies) and coverslipping. Images were acquired with a Leica DMRB microscope and DFC500 digital camera using Leica Application Suite v3.5.0 and then further analyzed using ImageJ software (NIH). We used fluorophore-conjugated secondary antibodies raised in goat against rabbit (1:1,000, Alexa Fluor 488; Life Technologies). Fos staining was performed 60 min after hind paw injection of BomoTx or PBS. Rabbit anti-Fos (Calbiochem) was used 1:30,000, followed by biotinylated goat anti-rabbit antibody (Vector Labs; 1:200), avidin–biotin conjugate, and nickel-enhanced diaminobenzidine detection (Vectastain ABC; Vector Labs). ATF3 antibody (Santa Cruz Biotechnology) was used at 1:2,000.

Cell-Death Assay. Primary sensory neurons or HEK293 cells were seeded at 50 μL, 30,000 cells per well in white opaque 96-well plates and incubated overnight at 37 °C in 5% CO_2. BomoTx was diluted with buffer (140 mM NaCl, 5 mM KCl, 2 mM $CaCl_2$, 2 mM $MgCl_2$, 10 mM glucose, 10 mM Hepes, pH 7.4) and delivered to cells for 5 min before luminogenic cell-impermeant peptide substrate (AAF-aminoluciferin) from CytoTox-Glo (Promega) was added to measure dead-cell protease activity. Lysis reagent was added at the end to induce cell death and to reveal total cells, as described in the manufacturer's instructions.

Statistics and Experiment Design. Data were analyzed using Prism 6 software (GraphPad Software), and significance testing used one-way analysis of variance (ANOVA) followed by post hoc Tukey's test, as noted in the figure legends. All significance tests are two-sided. Significance levels are $^{*}P < 0.05$, $^{**}P < 0.01$, $^{***}P < 0.001$, and $^{****}P < 0.0001$. The number of experiments (*n*) and significance are reported in the figure legends. Sample sizes for cellular physiology, histology, and animal behavior were chosen based on previous experience with these assays as the minimum number of independent observations required for statistically significant results. We assume equal variance and normally distributed data within experimental paradigms where comparisons are made. These are common assumptions relied upon for significance testing within these experimental paradigms as previously published by our group and others.

ACKNOWLEDGMENTS. We thank Thomas E. Finger (Department of Cell and Developmental Biology, University of Colorado School of Medicine) for generously providing the $P2X_2/P2X_3^{dbl-/-}$ mice; Stephanie A. Redmond and Jonah Chan (Department of Neurology, University of California, San Francisco) for discussions and kindly providing the embryonic DRG cultures; Katherine Hamel and João M. Bráz (Department of Anatomy, University of California, San Francisco) for technical assistance in behavioral experiments, discussions, and kindly providing the $PPTA^{-/-}$ mice; Jeannie Poblete, John V. King, Joshua J. Emrick, and members of the D.J. laboratory for technical assistance, discussions, and comments; and Gerhard P. Dahl (Department of Physiology and Biophysics, University of Miami) and Douglas A. Bayliss (Department of Pharmacology, University of Virginia) for pannexin constructs. We also thank Diana Bautista and Robert Edwards for insightful critiques of this work. This work is supported by the following NIH grants: R37 NS065071 and R01 NS081115 (to D.J.); 8P41 GM103481 (to the Bio-Organic Biomedical Mass Spectrometry Resource at UCSF, Director: A. L. Burlingame); 2P40OD010960-13 Viper Resource Grant (to E.E.S.); and R37NS014627 (to A.I.B.). Funding was also provided by a UCSF Research Resource Program Shared Equipment Award funded by the Chancellor.

1. Fry BG, et al. (2009) The toxicogenomic multiverse: Convergent recruitment of proteins into animal venoms. *Annu Rev Genomics Hum Genet* 10:483–511.
2. Julius D, Basbaum AI (2001) Molecular mechanisms of nociception. *Nature* 413(6852): 203–210.
3. Bohlen CJ, et al. (2011) A heteromeric Texas coral snake toxin targets acid-sensing ion channels to produce pain. *Nature* 479(7373):410–414.
4. Bohlen CJ, et al. (2010) A bivalent tarantula toxin activates the capsaicin receptor, TRPV1, by targeting the outer pore domain. *Cell* 141(5):834–845.
5. Cao E, Liao M, Cheng Y, Julius D (2013) TRPV1 structures in distinct conformations reveal activation mechanisms. *Nature* 504(7478):113–118.
6. Baconguis I, Bohlen CJ, Goehring A, Julius D, Gouaux E (2014) X-ray structure of acid-sensing ion channel 1-snake toxin complex reveals open state of a Na(+)-selective channel. *Cell* 156(4):717–729.
7. Osteen JD, et al. (2016) Selective spider toxins reveal a role for the $Na_v1.1$ channel in mechanical pain. *Nature* 534(7608):494–499.
8. Diochot S, et al. (2012) Black mamba venom peptides target acid-sensing ion channels to abolish pain. *Nature* 490(7421):552–555.
9. Gutierrez JM, Lomonte B (2013) Phospholipases A2: Unveiling the secrets of a functionally versatile group of snake venom toxins. *Toxicon* 62:27–39.
10. Cintra-Francischinelli M, et al. (2010) *Bothrops* snake myotoxins induce a large efflux of ATP and potassium with spreading of cell damage and pain. *Proc Natl Acad Sci USA* 107(32):14140–14145.
11. Fernandes CA, Borges RJ, Lomonte B, Fontes MR (2014) A structure-based proposal for a comprehensive myotoxic mechanism of phospholipase A2-like proteins from viperid snake venoms. *Biochim Biophys Acta* 1844(12):2265–2276.
12. Montecucco C, Gutiérrez JM, Lomonte B (2008) Cellular pathology induced by snake venom phospholipase A2 myotoxins and neurotoxins: Common aspects of their mechanisms of action. *Cell Mol Life Sci* 65(18):2897–2912.
13. Campbell JA, Lamar WW, Brodie ED (2004) *The Venomous Reptiles of the Western Hemisphere* (Comstock, Ithaca, NY).
14. Casewell NR, Wüster W, Vonk FJ, Harrison RA, Fry BG (2013) Complex cocktails: The evolutionary novelty of venoms. *Trends Ecol Evol* 28(4):219–229.
15. Jahangir A, et al. (2009) Identification and SAR of novel diaminopyrimidines. Part 2: The discovery of RO-51, a potent and selective, dual P2X(3)/P2X(2/3) antagonist for the treatment of pain. *Bioorg Med Chem Lett* 19(6):1632–1635.
16. Dahl G (2015) ATP release through pannexon channels. *Philos Trans R Soc Lond B Biol Sci* 370(1672):20140191.
17. Lewis C, et al. (1995) Coexpression of P2X2 and P2X3 receptor subunits can account for ATP-gated currents in sensory neurons. *Nature* 377(6548):432–435.
18. Mishra SK, Hoon MA (2010) Ablation of TrpV1 neurons reveals their selective role in thermal pain sensation. *Mol Cell Neurosci* 43(1):157–163.
19. Cavanaugh DJ, et al. (2009) Distinct subsets of unmyelinated primary sensory fibers mediate behavioral responses to noxious thermal and mechanical stimuli. *Proc Natl Acad Sci USA* 106(22):9075–9080.
20. Cockayne DA, et al. (2000) Urinary bladder hyporeflexia and reduced pain-related behaviour in P2X3-deficient mice. *Nature* 407(6807):1011–1015.
21. Cockayne DA, et al. (2005) P2X2 knockout mice and P2X2/P2X3 double knockout mice reveal a role for the P2X2 receptor subunit in mediating multiple sensory effects of ATP. *J Physiol* 567(Pt 2):621–639.
22. Idzko M, Ferrari D, Eltzschig HK (2014) Nucleotide signalling during inflammation. *Nature* 509(7500):310–317.
23. Cao YQ, et al. (1998) Primary afferent tachykinins are required to experience moderate to intense pain. *Nature* 392(6674):390–394.
24. Bland-Ward PA, Humphrey PP (1997) Acute nociception mediated by hindpaw P2X receptor activation in the rat. *Br J Pharmacol* 122(2):365–371.
25. Tsuda M, et al. (2000) Mechanical allodynia caused by intraplantar injection of P2X receptor agonist in rats: Involvement of heteromeric P2X2/3 receptor signaling in capsaicin-insensitive primary afferent neurons. *J Neurosci* 20(15):RC90.
26. Skals M, Jorgensen NR, Leipziger J, Praetorius HA (2009) Alpha-hemolysin from *Escherichia coli* uses endogenous amplification through P2X receptor activation to induce hemolysis. *Proc Natl Acad Sci USA* 106(10):4030–4035.
27. Belmonte G, et al. (1987) Pore formation by *Staphylococcus aureus* alpha-toxin in lipid bilayers. Dependence upon temperature and toxin concentration. *Eur Biophys J* 14(6): 349–358.
28. Chekeni FB, et al. (2010) Pannexin 1 channels mediate 'find-me' signal release and membrane permeability during apoptosis. *Nature* 467(7317):863–867.
29. Seminario-Vidal L, et al. (2011) Rho signaling regulates pannexin 1-mediated ATP release from airway epithelia. *J Biol Chem* 286(30):26277–26286.
30. Bao L, Locovei S, Dahl G (2004) Pannexin membrane channels are mechanosensitive conduits for ATP. *FEBS Lett* 572(1–3):65–68.
31. Nishioka SdeA, Silveira PV (1992) A clinical and epidemiologic study of 292 cases of lance-headed viper bite in a Brazilian teaching hospital. *Am J Trop Med Hyg* 47(6): 805–810.
32. Nishioka SA, Silveira PV, Peixoto-Filho FM, Jorge MT, Sandoz A (2000) Occupational injuries with captive lance-headed vipers (*Bothrops moojeni*): Experience from a snake farm in Brazil. *Trop Med Int Health* 5(7):507–510.
33. Bernardes CP, et al. (2008) Isolation and structural characterization of a new fibrin (ogen)olytic metalloproteinase from *Bothrops moojeni* snake venom. *Toxicon* 51(4): 574–584.
34. Sartim MA, et al. (2016) Moojenactivase, a novel pro-coagulant PIIId metalloprotease isolated from *Bothrops moojeni* snake venom, activates coagulation factors II and X and induces tissue factor up-regulation in leukocytes. *Arch Toxicol* 90(5):1261–1278.
35. de Oliveira F, et al. (2016) Biochemical and functional characterization of BmooSP, a new serine protease from *Bothrops moojeni* snake venom. *Toxicon* 111:130–138.
36. França SC, et al. (2007) Molecular approaches for structural characterization of *Bothrops* L-amino acid oxidases with antiprotozoal activity: cDNA cloning, comparative sequence analysis, and molecular modeling. *Biochem Biophys Res Commun* 355(2): 302–306.
37. Silveira LB, et al. (2013) Isolation and expression of a hypotensive and anti-platelet acidic phospholipase A2 from *Bothrops moojeni* snake venom. *J Pharm Biomed Anal* 73:35–43.
38. Soares AM, et al. (2000) Structural and functional characterization of myotoxin I, a Lys49 phospholipase A(2) homologue from *Bothrops moojeni* (Caissaca) snake venom. *Arch Biochem Biophys* 373(1):7–15.
39. Honore P, et al. (2002) Analgesic profile of intrathecal P2X(3) antisense oligonucleotide treatment in chronic inflammatory and neuropathic pain states in rats. *Pain* 99(1–2):11–19.
40. National Research Council (2011) *Guide for the Care and Use of Laboratory Animals* (The National Academies Press, Washington, DC), 8th Ed.